 doi:10.20944/preprints201904.0031.v1

Article

Transcriptome analysis of brain tissues in a MeCP2-null rat model of Rett syndrome

Liang Le[1], Hui Fu[1], Xue Bai[1], Caihong Lv[1], Wei Zhai[1], Baoping Jiang[1], Hai Gao[2*], Keping Hu[1*]

1. Institute of Medicinal Plant Development, Chinese Academy of Medical Sciences, Peking Union Medical College, Beijing 100193, China;
2. Institutes, of Biomedical Sciences, Fudan University, Shanghai 200032, China
***Corresponding authors:** Hai Gao, gaohai@fudan.edu.cn;
Keping Hu, kphu@implad.ac.cn

Keywords: *Rett syndrome;* MeCP2; transcriptome; MAPK signalling pathway; calcium ion signalling pathway

Abstract: Objective: Rett syndrome (RTT) is an X-linked neurodevelopmental disorder caused by mutations in *MeCP2*, a transcription factor. *MeCP2* mutations cause abnormal expression of downstream genes and eventually lead to brain dysfunction. The role of *MeCP2* in brain neural development remains unclear. To further elucidate this role, a *MeCP2*-null rat model was created with the CRISPR/cas9 system. **Method**: A *MeCP2*-cas9 vector was constructed and then microinjected into fertilized rat ova in vitro. Two mutations by CRISPR/cas9 were confirmed to cause deletions in exon 2 of *MeCP2* via DNA sequencing, and protein expression was measured by Western blotting. Transcriptome data for three brain tissues, the cerebellum, cerebral cortex and hippocampus, were obtained via next-generation sequencing. **Results**: *MeCP2*-null rats were successfully obtained, and preliminary analysis showed that the MeCP2-null rats exhibited motor dysfunction and anxious and depressed behaviour. In addition, differentially expressed genes (DEGs) were identified in the three MeCP2-null brain tissues compared to wild-type rat brain tissues. In the rat cerebellum, 388 downregulated DEGs were mainly involved in the calcium ion signalling pathway and the PI3K-Akt signalling pathway. In the cerebral cortex, 386 upregulated DEGs were primarily involved in intracellular signal transduction, protein phosphorylation and the MAPK signalling pathway. In the hippocampus, the DEGs were related to the MAPK signalling pathway. **Conclusion:** We constructed a *MeCP2*-null rat model with unique features with CRISPR/cas9 technology to study RTT and analysed DEGs in three rat brain tissues to highlight potential targets for the development of new medicines.

Keywords: Rett syndrome; *MeCP2*; CRISPR/cas9; transcriptome; calcium ion

1. Introduction

In 1966, Andreas Rett first described a brain atrophy-like symptom in girls [1]. Bengt Hagberg publicly reported the features of the disease in English and commemorated Andreas Rett by naming the disease Rett syndrome (RTT) in 1983 [2]. RTT mainly affects girls, with an incidence of approximately 0.01% among live female births. In typical RTT, patients show apparently normal psychomotor development for the first 6 months of life, followed by stagnation of development, slow growth of head circumference, autistic-like behaviour, mental retardation, motor dysfunction, irregular breathing and other behaviours. With growth, these children fail to meet psychomotor milestones and eventually regress, losing skill such as hand skills and spoken language skills [3]. In 1992, Adrian Bird discovered the *MeCP2* gene that encodes methyl-CpG-binding protein 2 *(MECP2)* [4]. More than 95% of typical RTT cases are caused by mutations in the gene encoding this transcriptional modulator [5, 6] .

 doi:10.20944/preprints201904.0031.v1

Many studies have focused on the function of MeCP2 in neurodevelopment and the mechanism of RTT. MeCP2 is a widespread DNA-binding protein. It has been reported that one MeCP2 molecule occupies 11 bp of DNA [7]. The MeCP2 protein contains a nuclear localization signal (NLS), a methyl-CPG-binding domain (MBD) and a transcriptional repression domain (TRD) [8]. Recent studies have found that MeCP2 can bind not only methylated DNA [9] but also non-methylated DNA [10]. Moreover, most MeCP2 binding sites are in intronic regions between transcription units and outside of CPG islands [11]. MeCP2 acts as a transcription inhibitor, and its TRD domain can bind to the AT-hook of the target gene to inhibit transcription [11-13]. MeCP2 can also recruit CBER to form a co-activator that activates the transcription of downstream genes [14]. Phosphorylation of MeCP2 protein can activate the expression of BDNF and play an important role in neurodevelopment [15, 16]. In addition, MeCP2 participates in the splicing of mRNA, thus affecting gene transcription [17].

RTT is a postnatal developmental disorder rather than a neurodegenerative disorder [18]. The mechanism of RTT remains unclear, although many studies have focused on MeCP2 and RTT. To study the role of MeCP2 in neurodevelopment, several mouse models of MeCP2 mutations have been constructed [19-22]. Recently, researchers have attempted to construct a MeCP2 transgenic monkey model that exhibits stereotyped behaviour and social disorders similar to those in human autism [23, 24]. Notably, that a majority of work in the field has focused on the loss of MeCP2 in male mice, which develop a condition similar to that observed in boys with MECP2 mutations [25]. However, in light of the fact that typical RTT is a female disorder, our understanding of the disease would benefit from further efforts to elucidate the complete spectrum of behavioural abnormalities in Mecp2-deficient female mice [3]. However, reliance on laboratory mice to identify viable therapies for human conditions may present challenges in translating findings from the bench to the clinic. Rats are widely used for disease models because they are physiologically closer to humans than are mice. Rat RTT models exhibit more similarities with typical RTT patients than do mouse RTT models [26]. Here, we report a novel Mecp2 rat model. Preliminary analysis of the phenotype of knockout (KO) rats in this experiment indicated that the phenotype was similar to that of RTT patients. We also analysed the transcriptome data of brain tissues in the rat model. The MeCP2-null genotype induced completely different expression patterns of different genes in the rat cerebellum, cortex and hippocampus.

2. Materials and Methods

2.1. Animal culture

Laboratory animals were fed ad libitum in a specific pathogen-free (SPF) animal laboratory and given free access to drinking water. Light and dark cycles were monitored, and the animal laboratory was maintained at room temperature (20-26°C) with a relative humidity of 40-70%.

The study was approved by the Ethics Committee of the Institute of Medicinal Plant Development, Chinese Academy of Medical Sciences and Peking Union Medical College (CAMS&PUMC, Beijing, China). All experimental procedures were performed in accordance with relevant guidelines approved by the Ethics Committee of the Institute of Medicinal Plant Development, CAMS&PUMC (laboratory animal licence: SCXK (Beijing) 2012-0001).

2.2. Generation of CRISPR-mediated MeCP2-KO rats

CRISPR-mediated MeCP2-KO rats were produced by Beijing ViewSolid Biotechnology (Beijing, China). The plasmid pCAG-T7-Cas9 was used as a transcription template in vitro after NotI restriction enzyme digestion and gel purification. Cas9 mRNA was transcribed with the mMESSAGE mMACHINE T7 Ultra Kit (Life Technologies). MeCP2-gRNA templates were amplified based on gRNA scaffolds using the T7 promoter sequence-conjugated primers T7-MeCP2-g4-FP and gRNA-RP (Table 1). MeCP2-gRNA was transcribed with a fast in vitro transcription T7 kit (Cat. VK010, Beijing ViewSolid Biotechnology, China) and frozen at −80°C. Zygotes of Sprague-Dawley (SD) rats were injected with a mixture of Cas9 mRNA and MeCP2-gRNA in M2 medium (Millipore) using a FemtoJet micromanipulator (Eppendorf, Germany). Then, the microinjected zygotes were transferred to pseudopregnant females for gestation. All rats were maintained in an SPF facility. DNA from the

 doi:10.20944/preprints201904.0031.v1

tails of two-week-old newborn rats was amplified with the primers MeCP2-sens and MeCP2-anti (Table 1) and sequenced. The genotypes of the mutant founder rats were obtained, and the founder rats were mated with wild-type (WT) SD rats to obtain heterozygous MeCP2$^{+/-}$ rats.

2.3. Animal behaviour observation

After birth, the weights and survival ratios of MeCP2-null rats were measured every day. After 9 weeks, the behaviour of at least five rats per group was analysed with the open field test and the step-through test. The total moving distance and the residence time in the central zone and marginal zone in the open field test were recorded. The residence time in the bright zone, the latency time and the error times in the step-through test were measured.

2.4. Off-target detection

For exon 2 of the MeCP2 gene in SD rats, potential off-target sites were predicted by Cas9 Target Design Software (http://crispr.mit.edu/), yielding a total of 25 off-target sites. The eleven potential off-target sites with the highest scores are listed in Table 2. The 25 predicted off-target sites were extended by 250 bp at the 5' and 3' ends to form off-target detection sequences (the lengths of the off-target detection sequences were 500-600 bp). Twenty-five pairs of off-target site detection primers were designed for the 25 off-target sequences. Genomic DNA was extracted and amplified from MeCP2-null rats by PCR and sequenced.

2.5. Total RNA preparation

Total RNA from MeCP2-null and WT rat cerebellum, cortex and hippocampus tissues was extracted by using TRIzol reagent (Invitrogen, Carlsbad, CA, USA) according to the manufacturer's instructions. RNA degradation and contamination were monitored on 1% agarose gels. RNA purity was checked using a NanoPhotometer spectrophotometer (Implen, CA, USA). RNA concentrations were measured using a Qubit® RNA Assay Kit with a Qubit 2.0 fluorometer (Life Technologies, CA, USA). RNA integrity was assessed using an RNA 6000 Nano kit (Agilent Technologies, CA, USA). A portion of the total RNA was used for RNA sequencing (RNA-seq), and the rest was reverse transcribed into first-strand cDNA using MMLV reverse transcriptase (Cat. # M1705, Promega, WI, USA), oligo(dT15) primers (Cat. # C1101, Promega, WI, USA) and a dNTP mixture (Cat. # U1515, Promega, WI, USA). The cDNA was stored at −20°C for real-time quantitative PCR (qRT-PCR) analysis.

2.6. RNA-seq and data analysis

An NEB Next Ultra™ RNA Library Prep kit (Illumina, San Diego, USA) was used to prepare sequencing libraries following the manufacturer's recommendations, and index codes were added to attribute the sequences to the appropriate samples. All samples (three samples per group) were sequenced (paired ends, 100 bp) on an Illumina HiSeq 4000 platform, and 125 bp/150 bp paired-end reads were generated. TopHat v2.0.12 was used to align the transcript sequences obtained from RNA-seq to the University of California, Santa Cruz (UCSC), reference genome rn6. Cufflinks software was then used to estimate the transcript levels (in fragments per kilobase of transcript per million mapped reads, FPKM) of the Refseq genes. Differentially expressed genes (DEGs) were identified using Cuffdiff with the default parameters of a $p<0.05$ and a 1.5-fold change between the two groups.

2.7. Gene ontology (GO) and Kyoto Encyclopedia of Genes and Genomes (KEGG) enrichment analyses of the DEGs

GO enrichment analysis of the DEGs was performed using the GOseq R package, which was also used to correct for gene length bias. DEGs were considered to be significantly enriched in GO categories that had corrected p values less than 0.01. We used KOBAS software to statistically test the enrichment of DEGs in KEGG pathways.

 doi:10.20944/preprints201904.0031.v1

2.8. Network analysis

A signed network was constructed using any genes that were expressed at FPKM values of 0.5 or higher in at least one sample. The soft-thresholding power was estimated and used to derive a pairwise distance matrix for selected genes using the topological overlap measure, and the dynamic hybrid cut method was used to detect clusters. Node centrality, defined as the sum of within-cluster connectivity measures, was used within each cluster to rank genes for "hubness." To visually analyse the constructed networks by hard thresholding of edge distances, the closest 150 edges were represented using Cytoscape 3.5.1.

2.9. qRT-PCR

cDNA was used as a template for PCR with qRT-PCR Master Mix (AQ101, Transgene, China). The reaction was performed in a thermal cycler (ABI StepOnePlus) at 94°C for 30 s followed by 40 cycles of 94°C for 5 s and 60°C for 30 s. The PCR primers are shown in Table 3. All samples were analysed in triplicate, and the gene expression levels were normalized to the β-actin values of the WT rats. Fold changes between the different groups were calculated using the $2^{-\Delta\Delta}$ cycle threshold method [27].

2.10. Protein extraction and Western blot assays

Total protein was extracted from rat cerebellum, cortex and hippocampus by homogenization in tissue protein extraction reagent (DE101, Transgene, China) with protease inhibitor cocktail (DI101, Transgene, China) and centrifugation (12000 × g) for 15 min at 4°C. The supernatants were collected, and the protein concentration was assayed with a BCA Protein Assay Kit (No. 23227, Thermo Scientific Pierce, Rockford). Western blot assays were performed as previously described. Briefly, equal amounts of protein were separated by sodium dodecyl sulfate-polyacrylamide gel electrophoresis (SDS-PAGE) and transferred to nitrocellulose membranes. The membranes were blocked in 4% non-fat milk before being incubated with diluted specific MeCP2 antibodies (Hu laboratory) [15, 28] at 4°C overnight. After five washes in Tris-buffered saline containing 0.1% Tween 20 (TBST), the membranes were incubated with a 1:5000 dilution of horseradish peroxidase-conjugated secondary antibodies in TBST for 1 h. The bands were detected by chemiluminescence detection reagents.

2.11. Statistical analysis

The data are expressed as the mean ± standard error of the mean (SEM). Statistical analysis was performed with one-way ANOVA using Prism 7 software (GraphPad, La Jolla, CA), and a least significant difference post hoc test was used to examine statistical significance ($p<0.05$ and $p<0.01$) between groups with multiple comparisons.

3. Results

3.1. Genotype identification of MeCP2-null rats

Using CRISPR-Cas9 technology, we first constructed a MeCP2-cas9 plasmid with the pCAG-T7-Cas9 plasmid to splice the rat MeCP2 exon 2 sequence (Fig. 1A, 1B). Then, microinjected zygotes were transferred to pseudopregnant females for gestation. DNA from the tails of two-week-old newborn rats was amplified by the MeCP2-sens and MeCP2-anti primers. A total of 20 pregnant female rats were obtained, and 100 fertilized eggs were collected. All of them were injected, and 10 rats were born (all female). Among them, 5 were positive MeCP2 gene KO rats (two genotypes), and 5 were WT rats, with a positive rate of 50%.

The genotypes of the rats were identified by MeCP2 gene sequencing. Five positive KO rats were detected, including three with the KO1 genotype and two with the KO2 genotype (Fig. 1C, 1D). The KO1 and KO2 genotypes featured 8 and 9 deleted bases, respectively (Fig. 1C). Both genotypes

Preprints (www.preprints.org) | NOT PEER-REVIEWED | Posted: 2 April 2019 doi:10.20944/preprints201904.0031.v1

resulted in frameshift mutations and induced errors in the amino acid sequence of the MeCP2 protein after EKSEDQ (exon 2) (Fig. 1C).

To verify the expression levels of MeCP2 protein in KO rats, Western blotting was used. The results showed that there was no expression of MeCP2 protein in the brain tissues of the KO rats with the two different genotypes, as shown in Figure 1E.

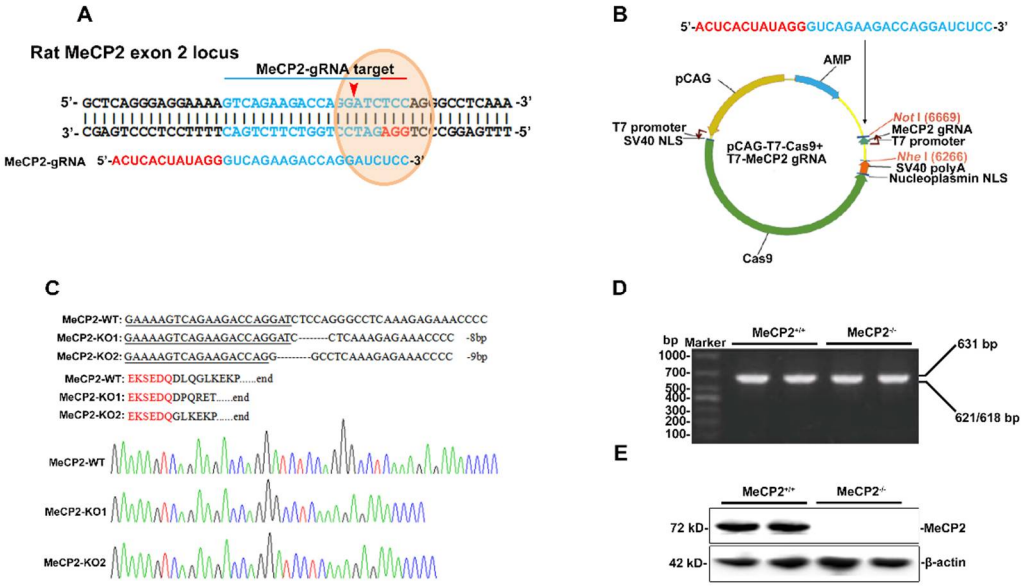

Figure 1. MeCP2 gene knockout rats. (A). Schematic of the *MeCP2* gene KO strategy in rats. Cas9 with a matching MeCP2-gRNA sequence targeted a locus within exon 2 of the rat *MeCP2* gene. (B). Plasmid map of pCAG-T7-Cas9+T7-MeCP2gRNA. (C). Detection of the two *MeCP2* gene mutations. (D). PCR amplification was used to identify 11- or 14-base deletions in exon 2 of the rat *MeCP2* gene. (E). Detection of MeCP2 by Western blot analysis.

Twenty-five potential off-target loci of two positive rats were sequenced, and the results were compared with WT sequences. The 11 potential off-target loci with the highest scores are listed in Table 2, and all of the loci are listed in the annex. No off-target mutations were detected.

3.2. Phenotypic and behavioural analysis of MeCP2-null rats

After successful establishment and identification of MeCP2-KO SD rats, positive female rats were selected (MeCP2 is located on the X chromosome; no male foetuses survived until birth) (Fig. 2A). The weights of all born rats were measured every week, and the weight difference between WT and KO rats was analysed. The results showed that there was a significant difference in weight between KO and WT rats ($p < 0.05$). The weight of the KO rats was significantly decreased eight weeks after birth (Fig. 2B). In addition, the death ratio of MeCP2-null rats was clearly higher than that of WT rats (Fig. 2C).

At 8 weeks after birth, the behavioural characteristics of the KO rats were analysed. The analysis methods included the open field test and the step-through test. The results of the open field test showed that the total distance for the KO group was less than that for the WT group (Fig. 2D). The residence times in the central area and marginal zone were significantly higher ($p < 0.05$) and lower ($p < 0.05$), respectively, for the KO rats than for the WT rats (Fig. 2E, 2F). In the step-through test, the residence time for MeCP2-null rats in the open area was significantly reduced ($p < 0.001$) (Fig. 2G), as was the latency ($p < 0.01$) (Fig. 2H), while the number of errors was increased ($p < 0.05$) (Fig. 2I).

Preprints (www.preprints.org) | NOT PEER-REVIEWED | Posted: 2 April 2019 doi:10.20944/preprints201904.0031.v1

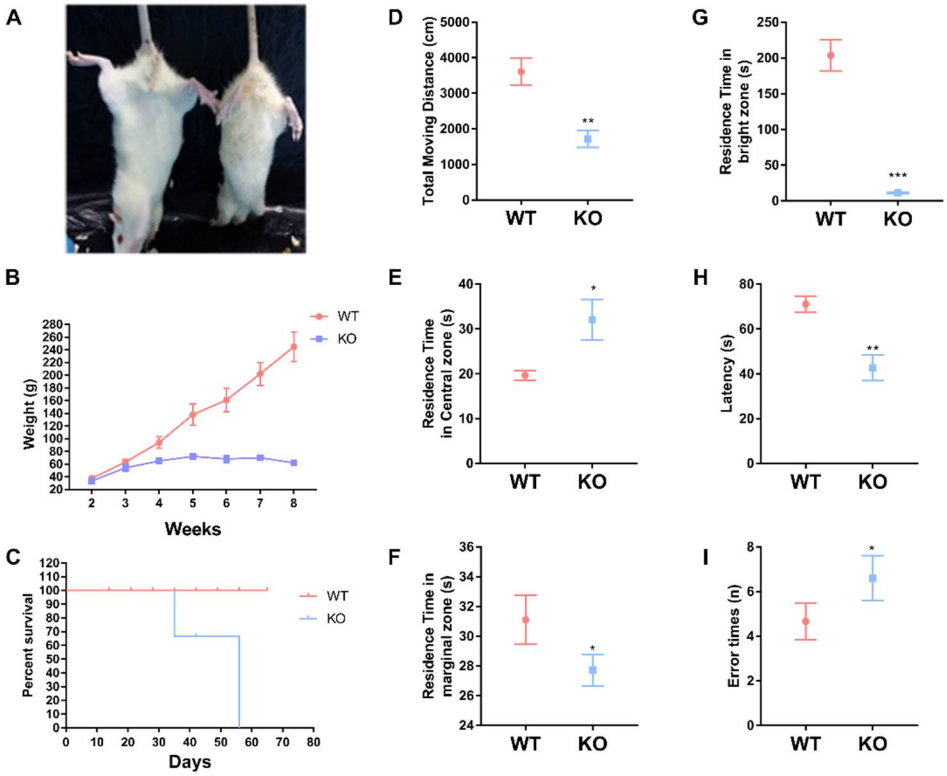

Figure 2. MeCP2 gene knockout induced motor dysfunction in rats. (A). Homozygous MeCP2$^{-/-}$ rats were shown. (B). Weights of MeCP2-null rats. (C). Survival rates of MeCP2-null rats. (D-F). The total moving distance (D) and the residence times in the central zone (E) and marginal zone (F) were measured in MeCP2-rats with an open field test. (G-I). The residence time in the bright zone (G), latency time (H) and error times (I) were measured in MeCP2-null rats with a step-through test. * $p <$ 0.05, ** $p < 0.01$, and *** $p < 0.0001$ vs. WT rats (n=5).

3.3. *Transcriptome analysis of MeCP2-null rat cerebellum tissue*

To study MeCP2 knockout-induced changes in the rat brain transcriptome, rat cerebellum, cortex and hippocampus tissues were collected for RNA-seq 9 weeks after birth. Rigorous bioinformatic and statistical approaches were used to analyse the RNA-seq data from the MeCP2-null and WT group samples. DEGs were identified upon comparison of the KO and WT groups (Fig. 3A). This experimental design allowed us to identify DEGs whose expression was changed by MeCP2 gene KO. A Venn diagram was constructed to show the overlapping DEGs among the cerebellum, cortex and hippocampus in the MeCP2-null rats compared with the WT rats. A total of 431, 425, and 194 genes were altered by MeCP2 KO in the cerebellum, cortex and hippocampus, respectively (Fig. 3A). Of those, 14, 10 and 17 DEGs overlapped between the cerebellum and cortex, the cerebellum and hippocampus, and the cortex and hippocampus, respectively (Fig. 3A). In the cerebellum, there were 455 DEGs (67 upregulated genes and 388 downregulated genes) in MeCP2-null rats compared to WT rats (Fig. 3B). In MeCP2-null rat cortex tissues, there were 456 DEGs (386 upregulated genes and 70 downregulated genes), while there were only 223 DEGs (127 upregulated genes and 96 downregulated genes) in the hippocampus (Fig. 3B). All DEGs in the three tissues were clustered and are shown in a heat map (Fig. 3C). MeCP2 KO primarily upregulated genes in the cerebellum and downregulated genes in the cortex. However, there were fewer DEGs in the hippocampus than in the other brain regions. Fourteen of the DEGs identified in the present study were expressed in both the cerebellum and cortex, including collagen type VI alpha 1 chain (Col6a1), UBX domain protein 2A (Ubxn2a), carboxypeptidase Z (Cpz), CD180 molecule (Cd180), multidrug resistance-associated protein 5 (Abcc5), peroxidasin (Pxdn) and Rab effector Noc2 (Rph3al; downregulated in the cerebellum but increased in the cortex), AABR07065923.1, otoferlin (Otof), transcription elongation factor A3 (Tcea3), hydroxycarboxylic acid receptor 2 (Hcar2), zinc finger protein 518B (Zfp518b;

Preprints (www.preprints.org) | NOT PEER-REVIEWED | Posted: 2 April 2019 doi:10.20944/preprints201904.0031.v1

downregulated in the cortex), collagen alpha-1 (V) chain (Col5a1) and period circadian protein homologue 1 (Per1) (Fig. 3D upper panel). Ten of the DEGs identified in the present study were expressed in both the cerebellum and hippocampus (Fig. 3D, middle panel), and 17 of the DEGs identified were expressed in both the cortex and hippocampus (Fig. 3D, lower panel).

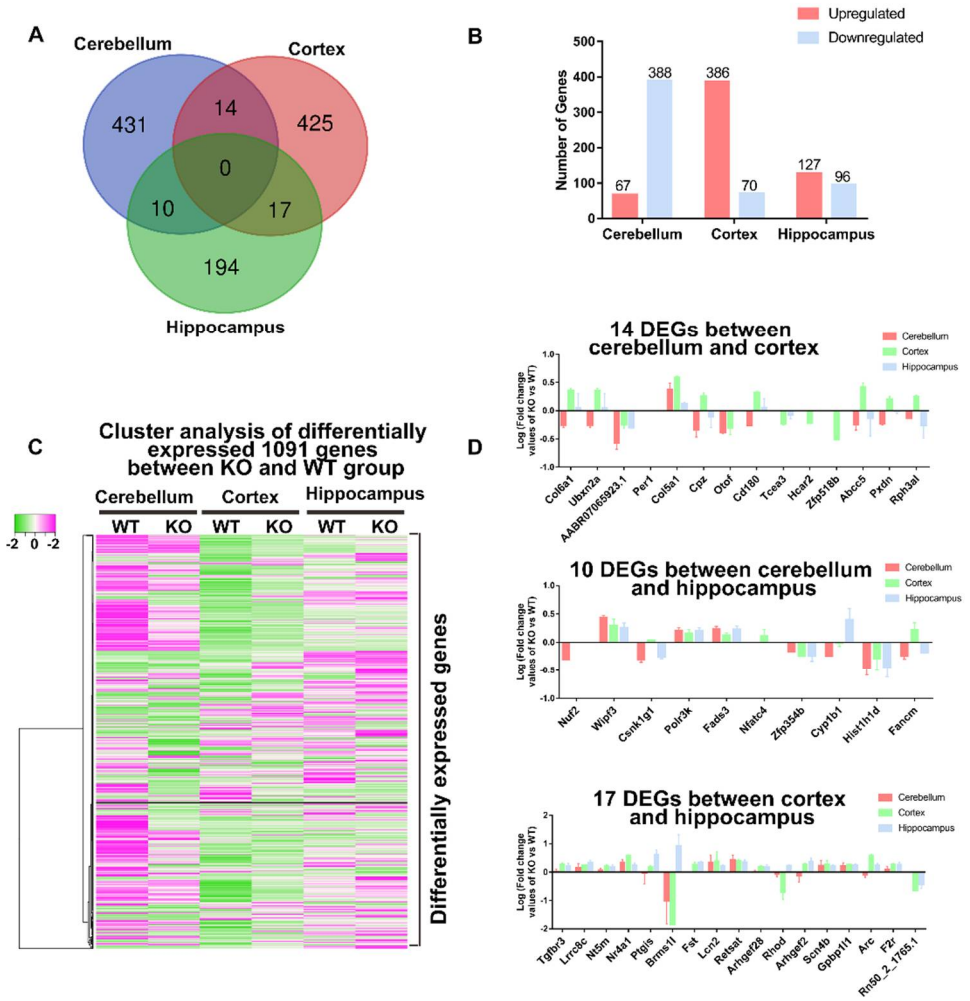

Figure 3. ***MeCP2*** **gene knockout alters rat brain tissue transcription.** Rat cerebellum, cortex and hippocampus tissues were collected and then subjected to RNA-seq gene expression analysis as described in the Materials and Methods. DEGs were identified in the MeCP2-null group compared with the WT group. (A) The Venn diagram shows the overlapping DEGs among the cerebellum, cortex and hippocampus tissues in MeCP2-null rats compared with WT rats. (B) The number of upregulated (orange-red) and downregulated (bright blue) genes in the MeCP2-null/WT categories in the rat cerebellum, cortex and hippocampus transcriptomes. (C). Heat map visualization of the results of cluster analysis of the 1091 DEGs that were significantly affected by MeCP2 gene knockout in the three brain tissues. (D). Changes in mRNA levels were determined as described in the Materials and Methods. The graphs shown the logarithm mean fold changes in the MeCP2-KO group normalized to the WT group values. Fourteen DEGs, 10 DEGs and 17 DEGs were shown to overlap between the cerebellum and cortex, cerebellum and hippocampus, and cortex and hippocampus, respectively (see Figure 1A).

In the MeCP2-null rat cerebellum tissues, 388 DEGs were downregulated and 67 DEGs were upregulated, as shown in the volcano plot (Fig. 3B, sFig. 1A). Functional enrichment was performed using Metacore™, and the results showed that the 388 downregulated DEGs were enriched in molecular function categories associated with extracellular matrix structural constituents, metal ion binding, integrin binding, platelet-derived growth factor binding, nucleic acid binding, serine-type carboxypeptidase activity, glycoprotein binding, and calcium ion binding. In KEGG pathway

Preprints (www.preprints.org) | NOT PEER-REVIEWED | Posted: 2 April 2019 doi:10.20944/preprints201904.0031.v1

analysis, the downregulated genes were associated with extracellular matrix (ECM)-receptor interactions, the PI3K-Akt signalling pathway, focal adhesion, protein digestion and absorption, amoebiasis, and the Ras signalling pathway (Fig. 4A). Network analysis of the DEGs that mapped to the GO term "metal ion binding and calcium ion binding" and that were known to directly interact showed that these genes encoded several members of the calcium ion binding pathway, such as adhesion G protein-coupled receptor E2 (*ADGRE1*), matrix metalloproteinase 19 (*MMP19*), EGF-containing fibulin-like extracellular matrix protein 1 (*EFEMP1*), protein jagged-1 (*JAG1*), matrix metalloproteinase 14 (*MMP14*), protein dachsous homologue 1 (*DCHS1*), and phospholipase A2 (*PLA2G2C*) (*Fig. 4B*). However, PI3K-Akt signalling pathway network analysis of the downregulated DEGs showed that MeCP2 KO downregulated receptor protein-tyrosine kinase (*EGFR*), fibroblast growth factor 14 (*FGF14*), fibroblast growth factor 20 (*FGF20*), integrin beta-4 (*ITGB4*), platelet-derived growth factor D (*PDGFD*), and kB kinase-associated protein 1 (*IKBKG*) in the cerebellum (Fig. 4C). Some other upregulated DEGs are listed in Figure 4D, such as transthyretin (TTR), a thyroid hormone-binding protein.

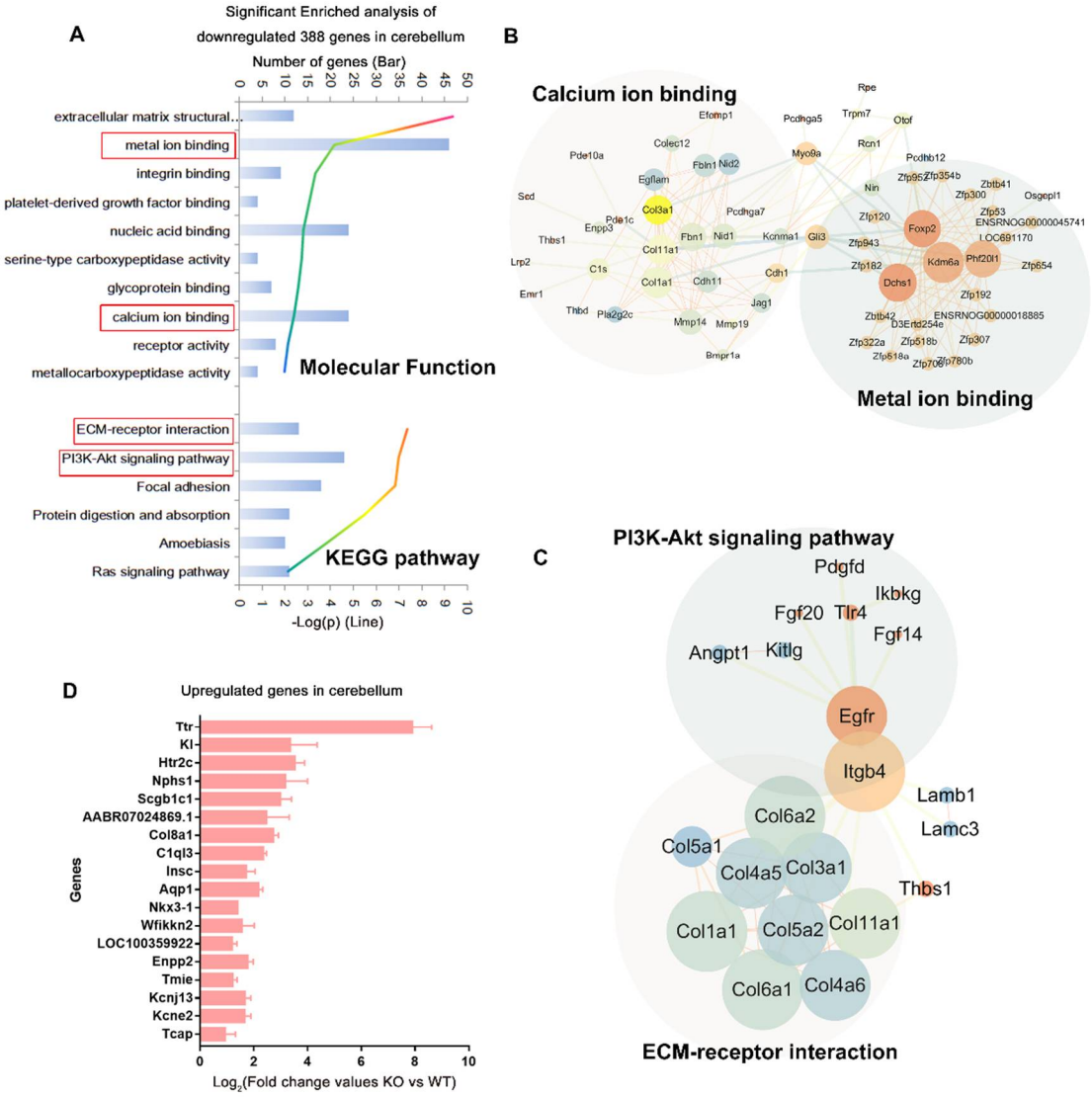

Figure 4. Genes significantly affected by MeCP2 gene knockout in the rat cerebellum. (A) Functional enrichment of the common downregulated DEGs with the highest FDR values in MeCP2-null rat cerebellum tissues. (B) The calcium ion binding and metal ion binding common gene network shows the enriched downregulated DEGs in the molecular function category. (C) The PI3K-Akt signalling pathway and ECM-receptor interaction common gene network shows the enriched downregulated DEGs in the KEGG pathway category. (D). The upregulated DEGs with the highest

 doi:10.20944/preprints201904.0031.v1

fold change values are listed. The graphs show the logarithm mean fold changes in the MeCP2-KO group normalized to the WT group values.

To validate the gene expression levels obtained from RNA-seq experiments, 10 downregulated genes involved in various molecular functions or KEGG pathway, including *FGF20, MMP19, EGFR, JAG1, MMP14, EFEMP1, FGF14, IKBKG, DCHS1,* and *ITGB4*, were selected for qRT-PCR. The qRT-PCR results were consistent with the RNA-seq data, except for *DCHS1* and *ITGB4* (sFig. 1B).

3.4. Transcriptome analysis of MeCP2-null rat cortex tissues

Unlike the cerebellum transcriptome, the MeCP2-null rat cortex transcriptome exhibited more upregulated genes and fewer downregulated genes, as shown in the volcano plot (Fig. 5A). The results of DEG functional enrichment analysis showed that the 386 upregulated DEGs were enriched in biological process categories associated with intracellular signal transduction, positive regulation of transcription from RNA, the polymerase II promoter, potassium ion transmembrane transport, protein phosphorylation, and other processes; in the molecular function category, the upregulated DEGs were associated with beta-catenin binding, Rho guanyl-nucleotide exchange factor activity, metal ion binding, PDZ domain binding, transcriptional repressor activity, RNA polymerase II core promoter proximal region sequence-specific binding, and transcription factor binding (Fig. 5B). Network analysis of the DEGs that mapped to the GO term “protein phosphorylation” showed that these genes encoded several proteins involved in inflammation and neurotrophin signalling, such as interleukin-1 receptor-associated kinase-like 2 (*IRAK2*), interleukin-1 receptor-associated kinase-like 1 (*IRAK1*), insulin-like growth factor 1 receptor (*IGF1R*), dual specificity mitogen-activated protein kinase kinase 7 (*MAP2K7*), mitogen-activated protein kinase kinase kinase 14 (*MAP3K14*), mitogen-activated protein kinase 15 (*MAPK15*), DEP domain-containing MTOR-interacting protein (*DEPTOR*), serine/threonine-protein kinase SIK1 (*SIK1*), connective tissue growth factor (*CTGF*), and transforming growth factor beta receptor type 3 (*TGFBR3*) (Fig. 5C). The downregulated genes with the lowest fold change values are listed in Figure 5D, such as BRMS1-like transcriptional repressor (Brms1l), which is associated with histone deacetylase (Fig. 5D).

Preprints (www.preprints.org) | NOT PEER-REVIEWED | Posted: 2 April 2019 doi:10.20944/preprints201904.0031.v1

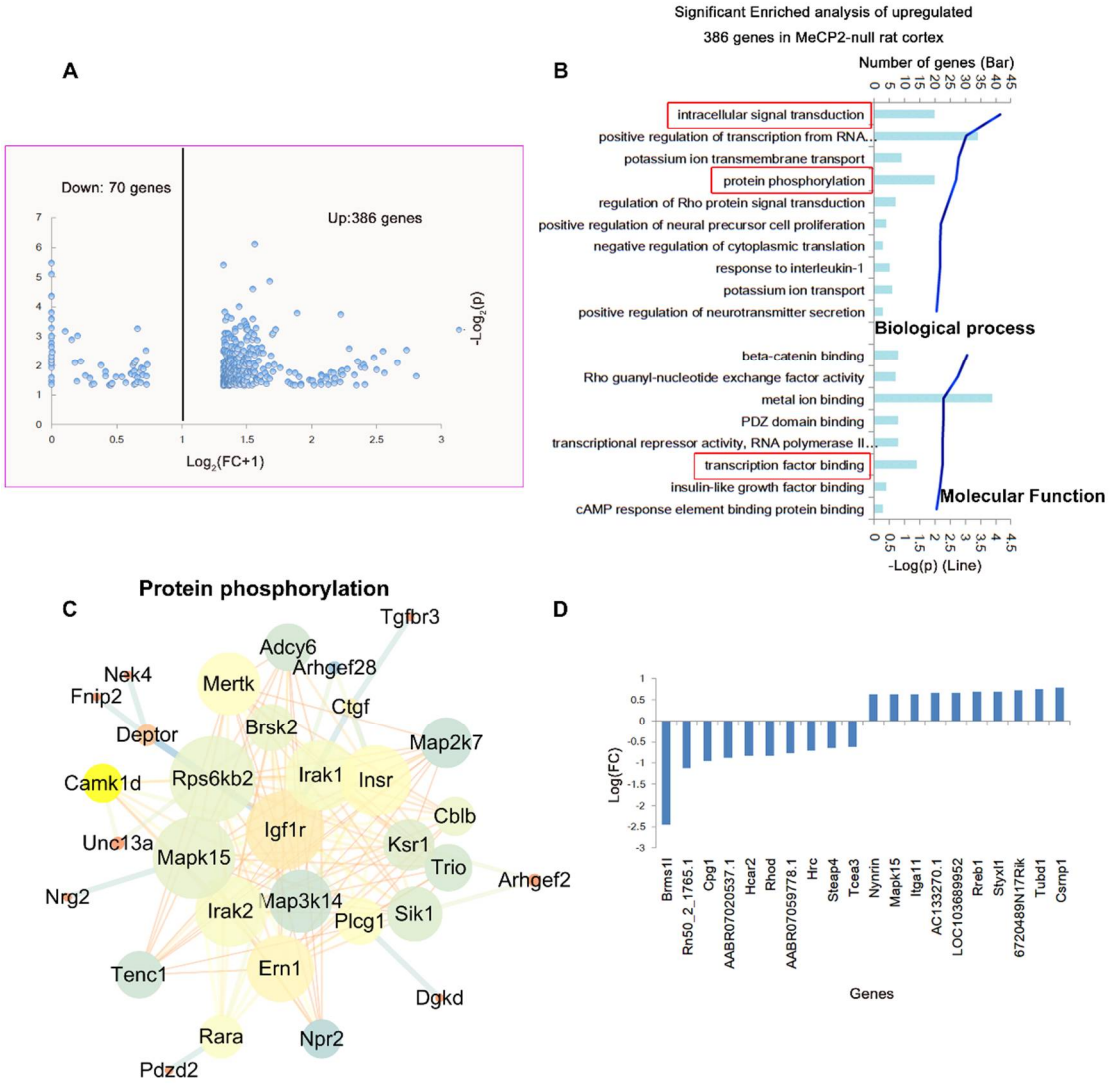

Figure 5. Genes significantly affected by MeCP2 gene knockout in the rat cortex. (A) Volcano plot showing the DEGs in the MeCP2-null rat cortex transcriptome. (B). Functional enrichment of the common upregulated DEGs with the highest FDR values in MeCP2-null rat cortex tissues. (C) The protein phosphorylation common gene network shows the enriched upregulated DEGs in the biological process category. (D). The DEGs with the lowest or highest fold change values are listed. The graphs show the logarithm mean fold changes in the MeCP2-KO group normalized to the WT group values.

The 14 upregulated genes NCOA2, *SUFU, PELP1, MED12, FOXO1, RBFOX2, RARA, DOT1L, PPP1R13B, TRERF1, EBF4, ZBTB49, PER1,* and *NR4A1*, which are involved in transcription factor binding, were selected for qRT-PCR. The qRT-PCR results were consistent with the RNA-seq data, except for *RARA and MED12* (sFig. 2).

3.5. *Transcriptome analysis of MeCP2-null rat hippocampus tissue*

The MeCP2-null rat hippocampus transcriptome exhibited fewer DEGs than the cerebellum and cortex transcriptomes, as shown in the volcano plot (Fig. 6A). Functional enrichment showed that these 127 upregulated DEGs were enriched for positive regulation of angiogenesis, regulation of Rho protein signal transduction, intracellular signal transduction, negative regulation of neuron apoptotic processes, regulation of actin cytoskeleton reorganization, and cell adhesion in the biological process category; for the endoplasmic reticulum, postsynaptic density, cytoskeleton, cell junction, perinuclear region of the cytoplasm, and MHC class I protein complex in the cellular component category; and for Rho guanyl-nucleotide exchange factor activity, protein kinase binding, and oxidoreductase

Preprints (www.preprints.org) | NOT PEER-REVIEWED | Posted: 2 April 2019 doi:10.20944/preprints201904.0031.v1

activity in the molecular function category (Fig. 6B). The upregulated DEGs were enriched for the MAPK signalling pathway in KEGG pathway analysis (Fig. 6B). The result of network analysis for all the DEGs are shown in Figure 6C. The high-impact upregulated DEGs in the network include Rhod, Rhob, MAPK4, PTK2B, CDKN1A, MAP3K5, GSK3A, TGFB2, and TGFBR3, while the high-impact downregulated DEGs include NOS3, CDKN3, TPM2, MYH11, NUF2, and CDCA8 (Fig. 6C).

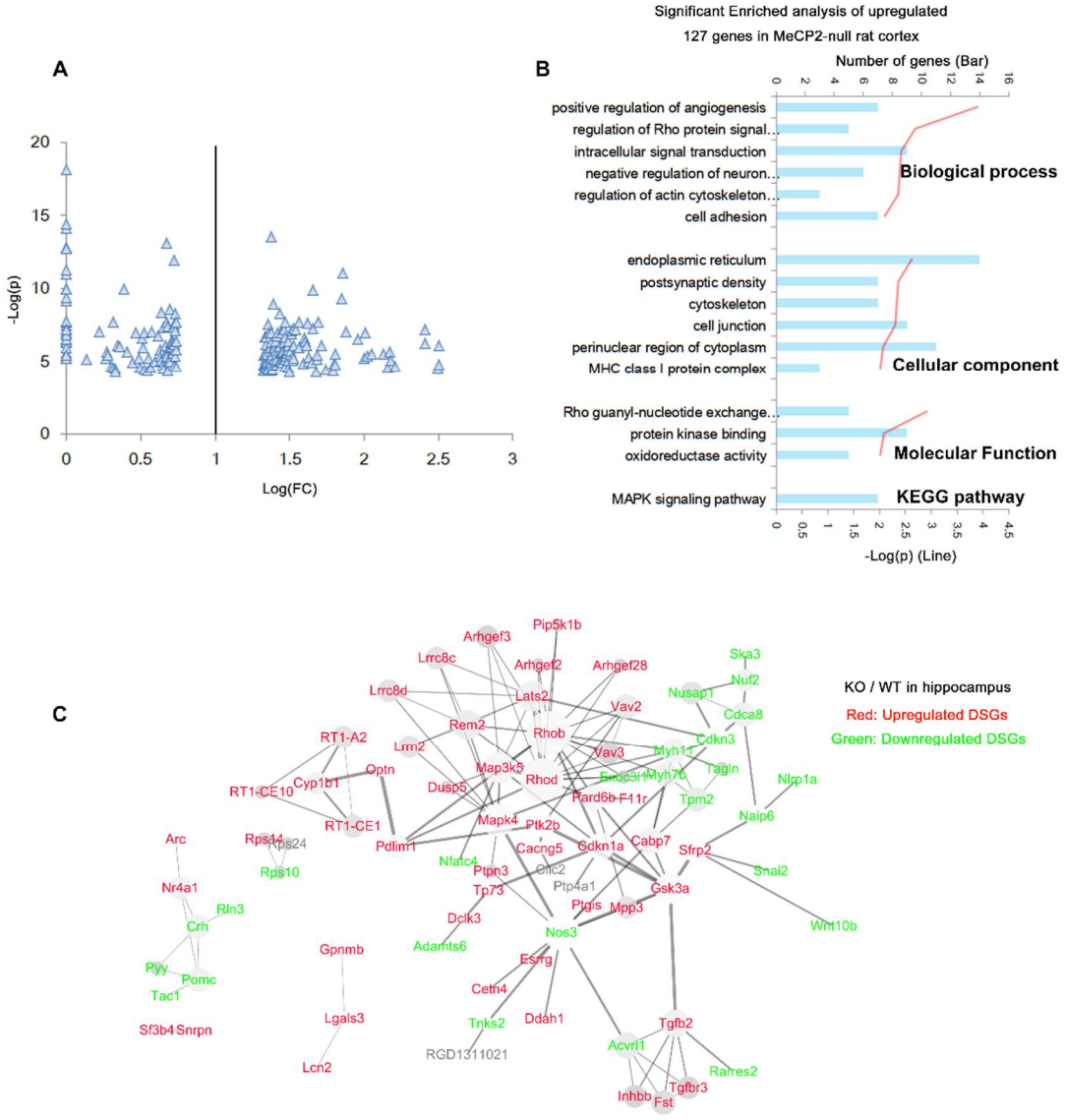

Figure 6. Genes significantly affected by MeCP2 gene knockout in the rat hippocampus. (A) Volcano plot showing the DEGs in the MeCP2-null rat hippocampus transcriptome. (B). Functional enrichment of the common upregulated DEGs with the highest FDR values in MeCP2-null rat cortex tissues. (C) All DEG interaction networks are shown. Red: DEGs upregulated in KO versus WT rats; green: downregulated DEGs.

4. Discussion

There have been many studies on the pathogenesis of RTT caused by MeCP2, but there has remained no suitable animal model. Compared with the homologous recombination method, the CRISPR/Cas9 system has the advantages of shorter cycles, lower cost and easier operation [29]. In this study, we constructed a MeCP2-null rat model with the CRISPR-Cas9 system. MeCP2 protein expression was completely absent in KO rat brain tissues (Fig. 1E).

Many studies on mouse models with MeCP2 deletions or mutations have not included behavioural analysis. In addition, the number of animals that can be produced with the homologous

 doi:10.20944/preprints201904.0031.v1

recombination method is limited, and the phenotypes of the resulting MeCP2-null mice do not entirely match those of typical RTT patients. In this study, the CRISPR/Cas9 system was used to obtain greater numbers of MeCP2-null rats simply and quickly, enabling the production of sufficient MeCP2 KO rats for behavioural analysis. Upon comparing the weights of KO rats and WT rats, it was found that the weights of MeCP2-null rats were significantly decreased at four weeks after birth, suggesting that KO of MeCP2 gradually affected the development of rats and then led to significant weight loss (Fig. 2B). There was also higher mortality of MeCP2-null rats than WT rats (Fig. 2C). The animal behavioural analyses included the open field test [30, 31] and the step-through test [32, 33]. The open field test is a way to observe neuropsychiatric changes in experimental animals that become evident when the animals enter open environments. When animals enter a new open environment, they tend to be more active at the edges and less active in the central area because of fear. However, the natural instincts of rats prompt them to investigate the central area, which leads to anxiety. The results showed that the total moving distance of KO rats was much shorter than that of WT rats. It may be that MeCP2 KO not only affected nerve development but also affected motor ability by affecting nerve-muscle junctions. There were significant differences in the number of shuttles and the residence time in the central area between KO rats and WT rats, clearly indicating that MeCP2 KO rats had anxious tendencies (Fig. 2D-F).

To understand the learning and memory abilities of MeCP2-null rats, a relatively simple passive avoidance conditioned reflex method (step-through test) was selected. The results showed that the bright zone residence time was significantly lower, the latency was lower, and the number of errors was higher in KO rats than in WT rats. These results indicated that MeCP2 KO rats had significant impairment of memory and cognition (Fig. 2G-I).

To explore the effects of MeCP2 on nerve development, we analysed the transcriptomes of three brain tissues (the cerebellum, cortex and hippocampus) using next-generation sequencing. There were very few overlapping DEGs among the three tissues (Fig. 3A), suggesting that MeCP2 KO affected the different brain tissues differently. In MeCP2-null rat cerebellum tissues, there were fivefold more downregulated genes than upregulated genes (Fig. 3B, sFig 1A). It is generally known that the cerebellum controls motor function [34]. These results indicate that the motor disability of MeCP2-null rats was associated with these downregulated DEGs in the cerebellum. A more detailed analysis showed that these genes were mainly involved in calcium ion binding (Fig. 4); such calcium-binding genes included *ADGRE1, MMP19, EFEMP1, JAG1, MMP14, DCHS1,* and *PLA2G2C*. Many studies have indicated that the function of MeCP2 in neurons is related to the calcium ion signalling pathway. Membrane depolarization triggers the calcium-dependent phosphorylation and release of MeCP2 from BDNF promoter III, thereby facilitating transcription [15, 35]. Nuclear calcium may also modulate the genome-wide chromatin state in response to synaptic activity via nuclear CaMKII-MeCP2 signalling [36]. KEGG pathway analysis indicated that the downregulated DEGs were mainly involved in ECM-receptor interactions and the PI3K-Akt signalling pathway (Fig. 4A, 4C). Neupane et al reported that MeCP2 splicing isoforms activate the major growth factor pathways targeted by activated RAS, the MAPK and PI3K-Akt pathways, and that MeCP2 overexpression activates the PI3K-Akt pathway [37]. Moreover, the low expression of *EGFR, FGF20,* and *FGF14* suggested that supplementation with these cellular growth factors may improve development in MeCP2-null rats. Russell et al reported that pretreatment with growth factor fibroblast growth factor 1 (FGF-1) partially protects MeCP2-/- cells [38]. Our transcriptome data suggest that the motor dysfunction caused by MeCP2 KO may be related to downregulation of the calcium ion signalling pathway and the PI3K-Akt signalling pathway in the rat cerebellum.

Unlike the cerebellum, the cerebral cortex is the largest site of neural integration in the central nervous system and plays a key role in memory, attention, perception, awareness, thought, language, and consciousness [39]. In our study, the results showed that MeCP2 KO induced more upregulated DEGs and fewer downregulated DEGs in the rat cerebral cortex than in the cerebellum (Fig. 3B, 5A). Indeed, the were fivefold more upregulated DEGs than downregulated DEGs. The upregulated DEGs were mainly involved in intracellular signal transduction protein phosphorylation processes and transcription factor binding (Fig. 5B). The upregulated DEGs

 doi:10.20944/preprints201904.0031.v1

involved in protein phosphorylation included *CAMK1D, IGF1R, IRAK1, SIK1, DEPTOR, TGFBR3, MAP2K7, MAPK15, MAP3K14, MERTK, RPS6KB2,* and *INSR*. Many studies have focused on the relationship between MAPK signalling and the function of MeCP2 [36, 40-44]. One previous study reported that the nuclear calcium-CaMKIV-CREB/CBP (cAMP-response element-binding protein/CREB-binding protein) pathway controls MeCP2 phosphorylation on S421 following synaptic activity [36]. Our previous study also showed that the shift in S80 and S421 phosphorylation on MeCP2 is controlled by calcium influx and CAMKK phosphorylation [15]. Mellios et al reported that miR-199 and miR-214, which are regulated by MeCP2, are increased during early brain development and differentially regulate extracellular signal-regulated kinase (ERK)/mitogen-activated protein kinase and protein kinase B (PKB/AKT) signalling [44]. Our transcriptome data for the cerebral cortex suggest that the overactivation of the MAPK signalling pathway in the MeCP2-null rat cortex may be related to nerve injury and anxious behaviour (Fig. 2D-F, 5B, 5C).

Interestingly, there were fewer DEGs induced by MeCP2 KO in the rat hippocampus, an important organ controlling learning and memory, than in the cerebellum and cerebral cortex. The number of DEGs in the hippocampus was half that in the two other brain tissues (Fig. 3B). In addition, the number of upregulated genes was almost the same as that of downregulated genes. The DEGs were involved in intracellular signal transduction, protein kinase binding, the MAPK signalling pathway, and other GO or KEGG pathway categories (Fig. 6B). The upregulated DEGs included *MAPK4, MAP3K5, GSK3α, and TGFB2*, which are involved in the MAPK signalling pathway (Fig. 6C). This finding suggests that the MAPK signalling pathway affects depressed behaviour in MeCP2-null rats in addition to anxious behaviour (Fig. 2). In addition, *NOS3* expression was significantly downregulated in the MeCP2-null rat hippocampus (Fig. 6C). Calmodulin-dependent protein kinase II alpha (CaMKIIα) has been shown to phosphorylate neuronal nitric oxide synthase (nNOS) at S847, resulting in a reduction in nNOS activity [45, 46]. Another study has provided evidence for an association between NOS3 mutation and social memory [47]. In a number of neuronal models of learning, signalling by the neurotransmitter nitric oxide (NO), which is synthesized by nNOS, has been found to be essential for the formation of long-term memory (LTM) [48]. Memory deficits in MeCP2-null rats may be related to the reduced expression of nNOS.

In conclusion, we successfully constructed a MeCP2-null rat model with CRISPR/cas9 technology. The behavioural characteristics of the resulting MeCP2-null rats were preliminarily explored. The cognition, memory and anxious tendencies of the KO rats were similar to those of patients with RTT syndrome; thus, this model provides a good tool for pharmacological research on RTT. The transcriptome data showed that there were different DEGs in the three MeCP2-null brain tissues (the cerebellum, cerebral cortex and hippocampus), suggesting that MeCP2 may have different functions in these tissues.

Funding: The work was supported by grants from the 973 Program (2013CB531200), CAMS Innovation Fund for Medical Sciences (CIFMS, 2016-I2M-1-002), National Natural Science Foundation of China (8010907 and 81271255).

Conflicts of Interest: The authors declare no conflict of interest.

References

1. Rett, A., [On a unusual brain atrophy syndrome in hyperammonemia in childhood]. *Wiener medizinische Wochenschrift* **1966,** 116, (37), 723-6.
2. Hagberg, B.; Aicardi, J.; Dias, K.; Ramos, O., A progressive syndrome of autism, dementia, ataxia, and loss of purposeful hand use in girls: Rett's syndrome: report of 35 cases. *Annals of neurology* **1983,** 14, (4), 471-9.
3. Samaco, R. C.; Neul, J. L., Complexities of Rett syndrome and MeCP2. *The Journal of neuroscience : the official journal of the Society for Neuroscience* **2011,** 31, (22), 7951-9.
4. Meehan, R. R.; Lewis, J. D.; Bird, A. P., Characterization of MeCP2, a vertebrate DNA binding protein with affinity for methylated DNA. *Nucleic acids research* **1992,** 20, (19), 5085-92.
5. Amir, R. E.; Van den Veyver, I. B.; Wan, M.; Tran, C. Q.; Francke, U.; Zoghbi, H. Y., Rett syndrome is caused by mutations in X-linked MECP2, encoding methyl-CpG-binding protein 2. *Nature genetics* **1999,** 23, (2), 185-8.

6. Neul, J. L.; Fang, P.; Barrish, J.; Lane, J.; Caeg, E. B.; Smith, E. O.; Zoghbi, H.; Percy, A.; Glaze, D. G., Specific mutations in methyl-CpG-binding protein 2 confer different severity in Rett syndrome. *Neurology* **2008,** 70, (16), 1313-21.
7. Ghosh, R. P.; Horowitz-Scherer, R. A.; Nikitina, T.; Shlyakhtenko, L. S.; Woodcock, C. L., MeCP2 binds cooperatively to its substrate and competes with histone H1 for chromatin binding sites. *Molecular and cellular biology* **2010,** 30, (19), 4656-70.
8. Quaderi, N. A.; Meehan, R. R.; Tate, P. H.; Cross, S. H.; Bird, A. P.; Chatterjee, A.; Herman, G. E.; Brown, S. D., Genetic and physical mapping of a gene encoding a methyl CpG binding protein, Mecp2, to the mouse X chromosome. *Genomics* **1994,** 22, (3), 648-51.
9. Nan, X.; Meehan, R. R.; Bird, A., Dissection of the methyl-CpG binding domain from the chromosomal protein MeCP2. *Nucleic acids research* **1993,** 21, (21), 4886-92.
10. Mellen, M.; Ayata, P.; Dewell, S.; Kriaucionis, S.; Heintz, N., MeCP2 binds to 5hmC enriched within active genes and accessible chromatin in the nervous system. *Cell* **2012,** 151, (7), 1417-30.
11. Baker, S. A.; Chen, L.; Wilkins, A. D.; Yu, P.; Lichtarge, O.; Zoghbi, H. Y., An AT-hook domain in MeCP2 determines the clinical course of Rett syndrome and related disorders. *Cell* **2013,** 152, (5), 984-96.
12. Zhou, X.; Liao, Y.; Xu, M.; Ji, Z.; Xu, Y.; Zhou, L.; Wei, X.; Hu, P.; Han, P.; Yang, F.; Pan, S.; Hu, Y., A novel mutation R190H in the AT-hook 1 domain of MeCP2 identified in an atypical Rett syndrome. *Oncotarget* **2017,** 8, (47), 82156-82164.
13. Xu, M.; Song, P.; Huang, W.; He, R.; He, Y.; Zhou, X.; Gu, Y.; Pan, S.; Hu, Y., Disruption of AT-hook 1 domain in MeCP2 protein caused behavioral abnormality in mice. *Biochimica et biophysica acta. Molecular basis of disease* **2018,** 1864, (2), 347-358.
14. Chahrour, M.; Jung, S. Y.; Shaw, C.; Zhou, X.; Wong, S. T.; Qin, J.; Zoghbi, H. Y., MeCP2, a key contributor to neurological disease, activates and represses transcription. *Science* **2008,** 320, (5880), 1224-9.
15. Tao, J.; Hu, K.; Chang, Q.; Wu, H.; Sherman, N. E.; Martinowich, K.; Klose, R. J.; Schanen, C.; Jaenisch, R.; Wang, W.; Sun, Y. E., Phosphorylation of MeCP2 at Serine 80 regulates its chromatin association and neurological function. *Proceedings of the National Academy of Sciences of the United States of America* **2009,** 106, (12), 4882-7.
16. Ebert, D. H.; Greenberg, M. E., Activity-dependent neuronal signalling and autism spectrum disorder. *Nature* **2013,** 493, (7432), 327-37.
17. Cheng, T. L.; Wang, Z.; Liao, Q.; Zhu, Y.; Zhou, W. H.; Xu, W.; Qiu, Z., MeCP2 suppresses nuclear microRNA processing and dendritic growth by regulating the DGCR8/Drosha complex. *Developmental cell* **2014,** 28, (5), 547-60.
18. Armstrong, D. D., Neuropathology of Rett syndrome. *Journal of child neurology* **2005,** 20, (9), 747-53.
19. Guy, J.; Hendrich, B.; Holmes, M.; Martin, J. E.; Bird, A., A mouse Mecp2-null mutation causes neurological symptoms that mimic Rett syndrome. *Nature genetics* **2001,** 27, (3), 322-6.
20. Chen, R. Z.; Akbarian, S.; Tudor, M.; Jaenisch, R., Deficiency of methyl-CpG binding protein-2 in CNS neurons results in a Rett-like phenotype in mice. *Nature genetics* **2001,** 27, (3), 327-31.
21. Shahbazian, M.; Young, J.; Yuva-Paylor, L.; Spencer, C.; Antalffy, B.; Noebels, J.; Armstrong, D.; Paylor, R.; Zoghbi, H., Mice with truncated MeCP2 recapitulate many Rett syndrome features and display hyperacetylation of histone H3. *Neuron* **2002,** 35, (2), 243-54.
22. Sztainberg, Y.; Chen, H. M.; Swann, J. W.; Hao, S.; Tang, B.; Wu, Z.; Tang, J.; Wan, Y. W.; Liu, Z.; Rigo, F.; Zoghbi, H. Y., Reversal of phenotypes in MECP2 duplication mice using genetic rescue or antisense oligonucleotides. *Nature* **2015,** 528, (7580), 123-6.
23. Liu, Z.; Zhou, X.; Zhu, Y.; Chen, Z. F.; Yu, B.; Wang, Y.; Zhang, C. C.; Nie, Y. H.; Sang, X.; Cai, Y. J.; Zhang, Y. F.; Zhang, C.; Zhou, W. H.; Sun, Q.; Qiu, Z., Generation of a monkey with MECP2 mutations by TALEN-based gene targeting. *Neuroscience bulletin* **2014,** 30, (3), 381-6.
24. Liu, Z.; Li, X.; Zhang, J. T.; Cai, Y. J.; Cheng, T. L.; Cheng, C.; Wang, Y.; Zhang, C. C.; Nie, Y. H.; Chen, Z. F.; Bian, W. J.; Zhang, L.; Xiao, J.; Lu, B.; Zhang, Y. F.; Zhang, X. D.; Sang, X.; Wu, J. J.; Xu, X.; Xiong, Z. Q.; Zhang, F.; Yu, X.; Gong, N.; Zhou, W. H.; Sun, Q.; Qiu, Z., Autism-like behaviours and germline transmission in transgenic monkeys overexpressing MeCP2. *Nature* **2016,** 530, (7588), 98-102.
25. Schule, B.; Armstrong, D. D.; Vogel, H.; Oviedo, A.; Francke, U., Severe congenital encephalopathy caused by MECP2 null mutations in males: central hypoxia and reduced neuronal dendritic structure. *Clinical genetics* **2008,** 74, (2), 116-26.
26. Veeraragavan, S.; Wan, Y. W.; Connolly, D. R.; Hamilton, S. M.; Ward, C. S.; Soriano, S.; Pitcher, M. R.;

McGraw, C. M.; Huang, S. G.; Green, J. R.; Yuva, L. A.; Liang, A. J.; Neul, J. L.; Yasui, D. H.; LaSalle, J. M.; Liu, Z.; Paylor, R.; Samaco, R. C., Loss of MeCP2 in the rat models regression, impaired sociability and transcriptional deficits of Rett syndrome. *Hum Mol Genet* **2016,** 25, (15), 3284-3302.

27. Livak, K. J.; Schmittgen, T. D., Analysis of relative gene expression data using real-time quantitative PCR and the 2(-Delta Delta C(T)) Method. *Methods* **2001,** 25, (4), 402-8.
28. Hu, K.; Nan, X.; Bird, A.; Wang, W., Testing for association between MeCP2 and the brahma-associated SWI/SNF chromatin-remodeling complex. *Nature genetics* **2006,** 38, (9), 962-4; author reply 964-7.
29. Ran, F. A.; Cong, L.; Yan, W. X.; Scott, D. A.; Gootenberg, J. S.; Kriz, A. J.; Zetsche, B.; Shalem, O.; Wu, X.; Makarova, K. S.; Koonin, E. V.; Sharp, P. A.; Zhang, F., In vivo genome editing using Staphylococcus aureus Cas9. *Nature* **2015,** 520, (7546), 186-91.
30. Badowska-Szalewska, E.; Ludkiewicz, B.; Sidor-Kaczmarek, J.; Lietzau, G.; Spodnik, J. H.; Swietlik, D.; Domaradzka-Pytel, B.; Morys, J., Hippocampal interleukin-1beta in the juvenile and middle-aged rat: response to chronic forced swim or high-light open-field stress stimulation. *Acta neurobiologiae experimentalis* **2013,** 73, (3), 364-78.
31. Baez, M. V.; Oberholzer, M. V.; Cercato, M. C.; Snitcofsky, M.; Aguirre, A. I.; Jerusalinsky, D. A., NMDA receptor subunits in the adult rat hippocampus undergo similar changes after 5 minutes in an open field and after LTP induction. *PloS one* **2013,** 8, (2), e55244.
32. Micale, V.; Cristino, L.; Tamburella, A.; Petrosino, S.; Leggio, G. M.; Di Marzo, V.; Drago, F., Enhanced cognitive performance of dopamine D3 receptor "knock-out" mice in the step-through passive-avoidance test: assessing the role of the endocannabinoid/endovanilloid systems. *Pharmacological research : the official journal of the Italian Pharmacological Society* **2010,** 61, (6), 531-6.
33. Darbra, S.; Balada, F.; Marti-Carbonell, M. A.; Garau, A., Perinatal hypothyroidism effects on step-through passive avoidance task in rats. *Physiology & behavior* **2004,** 82, (2-3), 497-501.
34. Honda, T.; Nagao, S.; Hashimoto, Y.; Ishikawa, K.; Yokota, T.; Mizusawa, H.; Ito, M., Tandem internal models execute motor learning in the cerebellum. *Proceedings of the National Academy of Sciences of the United States of America* **2018,** 115, (28), 7428-7433.
35. Chen, W. G.; Chang, Q.; Lin, Y.; Meissner, A.; West, A. E.; Griffith, E. C.; Jaenisch, R.; Greenberg, M. E., Derepression of BDNF transcription involves calcium-dependent phosphorylation of MeCP2. *Science* **2003,** 302, (5646), 885-9.
36. Buchthal, B.; Lau, D.; Weiss, U.; Weislogel, J. M.; Bading, H., Nuclear calcium signaling controls methyl-CpG-binding protein 2 (MeCP2) phosphorylation on serine 421 following synaptic activity. *The Journal of biological chemistry* **2012,** 287, (37), 30967-74.
37. Neupane, M.; Clark, A. P.; Landini, S.; Birkbak, N. J.; Eklund, A. C.; Lim, E.; Culhane, A. C.; Barry, W. T.; Schumacher, S. E.; Beroukhim, R.; Szallasi, Z.; Vidal, M.; Hill, D. E.; Silver, D. P., MECP2 Is a Frequently Amplified Oncogene with a Novel Epigenetic Mechanism That Mimics the Role of Activated RAS in Malignancy. *Cancer discovery* **2016,** 6, (1), 45-58.
38. Russell, J. C.; Blue, M. E.; Johnston, M. V.; Naidu, S.; Hossain, M. A., Enhanced cell death in MeCP2 null cerebellar granule neurons exposed to excitotoxicity and hypoxia. *Neuroscience* **2007,** 150, (3), 563-74.
39. Fernandez, V.; Llinares-Benadero, C.; Borrell, V., Cerebral cortex expansion and folding: what have we learned? *The EMBO journal* **2016,** 35, (10), 1021-44.
40. Alvarez-Saavedra, M.; Saez, M. A.; Kang, D.; Zoghbi, H. Y.; Young, J. I., Cell-specific expression of wild-type MeCP2 in mouse models of Rett syndrome yields insight about pathogenesis. *Hum Mol Genet* **2007,** 16, (19), 2315-25.
41. Jiang, Y.; Matevossian, A.; Guo, Y.; Akbarian, S., Setdb1-mediated histone H3K9 hypermethylation in neurons worsens the neurological phenotype of Mecp2-deficient mice. *Neuropharmacology* **2011,** 60, (7-8), 1088-97.
42. Zhao, L. Y.; Zhang, J.; Guo, B.; Yang, J.; Han, J.; Zhao, X. G.; Wang, X. F.; Liu, L. Y.; Li, Z. F.; Song, T. S.; Huang, C., MECP2 promotes cell proliferation by activating ERK1/2 and inhibiting p38 activity in human hepatocellular carcinoma HEPG2 cells. *Cellular and molecular biology* **2013,** Suppl 59, OL1876-81.
43. Tao, H.; Yang, J. J.; Hu, W.; Shi, K. H.; Deng, Z. Y.; Li, J., MeCP2 regulation of cardiac fibroblast proliferation and fibrosis by down-regulation of DUSP5. *International journal of biological macromolecules* **2016,** 82, 68-75.
44. Mellios, N.; Feldman, D. A.; Sheridan, S. D.; Ip, J. P. K.; Kwok, S.; Amoah, S. K.; Rosen, B.; Rodriguez, B. A.; Crawford, B.; Swaminathan, R.; Chou, S.; Li, Y.; Ziats, M.; Ernst, C.; Jaenisch, R.; Haggarty, S. J.; Sur, M., MeCP2-regulated miRNAs control early human neurogenesis through differential effects on ERK and AKT

565 signaling. *Molecular psychiatry* **2018,** 23, (4), 1051-1065.
566 45. Makino, K.; Osuka, K.; Watanabe, Y.; Usuda, N.; Hara, M.; Aoyama, M.; Takayasu, M.; Wakabayashi, T.,
567 Increased ICP promotes CaMKII-mediated phosphorylation of neuronal NOS at Ser(8)(4)(7) in the
568 hippocampus immediately after subarachnoid hemorrhage. *Brain research* **2015,** 1616, 19-25.
569 46. Komeima, K.; Hayashi, Y.; Naito, Y.; Watanabe, Y., Inhibition of neuronal nitric-oxide synthase by calcium/
570 calmodulin-dependent protein kinase IIalpha through Ser847 phosphorylation in NG108-15 neuronal cells.
571 *The Journal of biological chemistry* **2000,** 275, (36), 28139-43.
572 47. Henningsson, S.; Zettergren, A.; Hovey, D.; Jonsson, L.; Svard, J.; Cortes, D. S.; Melke, J.; Ebner, N. C.;
573 Laukka, P.; Fischer, H.; Westberg, L., Association between polymorphisms in NOS3 and KCNH2 and social
574 memory. *Frontiers in neuroscience* **2015,** 9, 393.
575 48. Korneev, S. A.; Straub, V.; Kemenes, I.; Korneeva, E. I.; Ott, S. R.; Benjamin, P. R.; O'Shea, M., Timed and
576 targeted differential regulation of nitric oxide synthase (NOS) and anti-NOS genes by reward conditioning
577 leading to long-term memory formation. *The Journal of neuroscience : the official journal of the Society for*
578 *Neuroscience* **2005,** 25, (5), 1188-92.
579
580